A DFT Study of the 1,3-Dipolar Cycloadditions on the C(100)-2 × 1 Surface

Xin Lu,* Xin Xu, Nanqin Wang, and Qianer Zhang

State Key Laboratory for Physical Chemistry of Solid Surfaces & Department of Chemistry, Xiamen University, Xiamen 361005, China

xinlu@xmu.edu.cn

Received September 13, 2001

The 1,3-dipolar cycloadditions (1,3-DCs) of a series of 1,3-dipolar molecules onto the C(100)-2 × 1 surface have been investigated by means of hybrid density functional B3LYP method in combination with cluster model approach. It was found that 1,3-DCs on the C(100)-2 × 1 surface are more favorable over their molecular analogues both thermodynamically and kinetically. The enhancement of the reactivity on the surface due to the reduced overlap between the p_π orbitals of the surface C═C dimer should be important for the semiconductor industry because it might lead to a breakthrough in the fabrication of diamond films at low temperature.

Introduction

Diamond is promising as an electronic-device material owing to its superlative optical, mechanical, and electronic properties such as high hardness, a large band gap, high saturation carrier velocity, and high thermal conductivity.[1−4] The chemical modification of diamond surfaces might introduce new physical and chemical properties for specific applications, e.g., metallization,[5] surface conductivity,[6−8] and electron emission.[9−11] Accordingly, it is of interest to explore the chemistry of the diamond surface and to seek specific ways of making controlled chemical modifications of diamond surfaces. In this paper, we report a systematic theoretical investigation of 1,3-dipolar cycloaddition (1,3-DC) reactions between 1,3-dipoles and the C(100)-2 × 1 surface. Our results indicate that 1,3-DC might be a new type of surface reactions that can be used to functionalize the diamond surface at low temperature.

The reconstructed C(100)-2 × 1 surface has a bonding motif where the adjacent surface carbon atoms are paired up to form symmetric dimers.[12,13] The bonding within the surface dimer can be described in terms of a strong σ bond and a weaker π bond, analogous to the bonding within the C═C double bond of simple alkenes. This implies the chemistry of the C(100)-2 × 1 surface might show some similarity to the chemistry of simple alkenes. Furthermore, due to the nonplanar geometry on the surface dimer, the overlap between the p_π orbitals of the surface dimer is reduced, and consequently, the π-bonding within the surface dimer is weaker than that in ethylene, giving rise to the possibility of a higher reactivity of the surface dimer. Indeed, previous experimental and theoretical studies revealed that on the C(100)-2 × 1 surface, a surface dimer, working as a dienophile, undergoes Diels−Alder cycloaddition reaction with an incoming conjugated diene (1,3-butadiene) to form a six-membered ring surface species,[14−17] and analogous surface reaction occurs readily on the Si(100) and Ge(100) surfaces,[18−23] which exhibit similar 2 × 1 reconstructions. This surface reaction is similar to, but more facile than, its well-known molecular precedent, i.e., Diels−Alder cycloaddition reaction between a simple alkene and a conjugated diene.[24] Needless to say, the latter is remarkably useful and has been widely employed in modern organic synthesis.

Apart from the famous Diels−Alder cycloaddition reactions, another class of pericyclic reactions in organic chemistry is the so-called 1,3-diploar cycloaddition (1,3-

* To whom correspondence should be addressed. Tel: +86-592-2181600. Fax: +86-592-2183047.

(1) Hossain, Z.; Kubo, T.; Aruga, T.; Takagi, N.; Tsuno, T.; Fujimori, N.; Nishijima, M. *Jpn. J. Appl. Phys.* **1999**, *38*, 6659.
(2) Ashfold, M. N. R.; May, P. W.; Rego, C. A.; Everitt, N. M. *Chem. Soc. Rev.* **1994**, *23*, 21.
(3) *MRS Bulletin*; Fleischer, E. L., Ed.; Materials Research Society: Warrendale, PA, 1998; p 23.
(4) *The Properties of Natural and Synthetic Diamond;* Field, J. E., Ed.; Academic Press: London, 1992.
(5) Potochnik, S. J.; Pehrsson, P. E.; Hsu, D. S.; Calvert, J. M. *Langmuir* **1995**, *11*, 1841.
(6) Grot, S. A.; Gildenblat, G. Sh.; Wronski, C. R.; Badzian, A. R.; Badzian, T.; Messier, R. *IEEE Elec. Dev. Lett.* **1990**, *11*, 100.
(7) Nakahata, H.; Imai, T.; Fujimori, N. *Diamond Materials, Proc. Vol. 98−8*; The Electrochemical Society; Pennington, NJ, 1991; p 487.
(8) Mackey, B. L.; Russell, J. N., Jr.; Crowell, J. E.; Butler, J. E. *Phys. Rev. B* **1995**, *52*, 17009.
(9) Malta, D. P.; Posthill, J. B.; Humphreys T. P.; Thomas, R. E.; Fountain, G. G.; Rudder, R. A.; Mantini, M. J.; Markuna, R. J. *Appl. Phys. Lett.* **1994**, *64*, 1929.
(10) Pickett, W. E. *Phys. Rev. Lett.* **1994**, *73*, 1664.
(11) van der Weide, J.; Nemanich, R. J. *J. Vac. Sci. Technol. B* **1994**, *12*, 2475.
(12) Krüger, P.; Pollmann, J. *Phys. Rev. Lett.* **1995**, *74*, 1155.
(13) Furthmüller, J.; Hafner, J.; Kresse, G. *Phys. Rev. B* **1996**, *53*, 7334.
(14) Wang G. T.; Bent, S. F.; Russell, J. N., Jr.; Butler, J. E.; D'Evelyn, M. P. *J. Am. Chem. Soc.* **2000**, *122*, 744.
(15) Hossain, Z.; Aruga, T.; Takagi, N.; Tsuno, T.; Fujimori, N.; Ando, T.; Nishijima, M. *Jpn. J. Appl. Phys.* **1999**, *38*, L1496.
(16) Fitzgerald D. R.; Doren D. J. *J. Am. Chem. Soc.* **2000**, *122*, 12334.
(17) Okamoto, Y. *J. Phys. Chem. B* **2001**, *105*, 1813.
(18) Konecny, R.; Doren, D. J. *J. Am. Chem. Soc.* **1997**, *119*, 11098.
(19) Konecny, R.; Doren, D. J. *Surf. Sci.* **1998**, *417*, 169.
(20) Teplyakov, A. V.; Kong, M. J.; Bent, S. F. *J. Am. Chem. Soc.* **1997**, *119*, 11100.
(21) Teplyakov, A. V.; Kong, M. J.; Bent, S. F. *J. Chem. Phys.* **1998**, *108*, 11100.
(22) Hovis, J. S.; Liu, H.; Hamers, R. J. *J. Phys. Chem. B* **1998**, *102*, 6873.
(23) Choi, C. H., Gordon, M. S. *J. Am. Chem. Soc.* **1999**, *121*, 11311.
(24) See, for example, Houk, K. N.; Li, Y.; Evanseck, J. D. *Angew. Chem., Int. Ed. Engl.* **1992**, *31*, 682.

10.1021/jo016114q CCC: $22.00
Published on Web 12/27/2001

DC) reaction.[25] The 1,3-DC is the union of a 1,3-dipolar molecule with a multiple bond system (a dipolarophile). The 1,3-dipole is a triad of atoms that has a π system of four electrons and can be represented by a zwitterionic octet resonance structure.[25] The great majority of 1,3-dipoles are isoelectronic with either 16- (e.g., diazomethane) or 18-valence-electron (e.g., ozone) compounds. The dipolarophiles are usually olefins or acetylenes, but other multiple bonds, such as the C═N bond of imines and the C═O bond of aldehyde, also can act as dipolarophiles.[25,26] Considering the weaker π-bonding within the surface dimer on the C(100)-2 × 1 surface, one infers that with the surface dimer working as a dipolarophile, analogous 1,3-DC reactions would occur between 1,3-dipolar molecules and the surface dimer and such surface 1,3-DC reactions should require lower activation energies than do their molecular analogues. This type of surface reactions, if facile, in combination with the large variety of 1,3-dipoles should be very useful for the functionalization of the diamond(100) surface at low temperature. It is noteworthy that analogous 1,3-DC reactions have been successfully employed to functionalize the highly conjugated C60 and C70 fullerenes,[27] and recent DFT studies predicted that 1,3-dipoles should strongly adsorb to the Si(100)-2 × 1 surface without a significant activation barrier.[28,29]

To confirm the above inference, we have systematically investigated the 1,3-DC reactions of a series of 1,3-dipolar molecules with the C(100)-2 × 1 surface by means of first-principle density functional (DFT) cluster model calculations. The 1,3-dipoles considered are those 16-valence-electron ones including nitrile ylide ($HCNCH_2$), nitrile imine (HCNNH), nitrile oxide (HCNO), diazomethane (H_2CNN), methyl azide (CH_3NNN), and nitrous oxide (N_2O) and those 18-valence-electron ones including nitromethane (CH_3NO_2) and ozone (O_3). In addition, the gas-phase 1,3-DC reactions of these 1,3-dipoles with ethylene have also been studied and compared with the surface reactions. The results clearly revealed the facileness of the surface reactions as well as a large enhancement of 1,3-DC reactivity on the surface.

Computational Details

The hybrid density functional theory B3LYP method, i.e., Becke's three-parameter nonlocal exchange functional[30] with the correlation functional of Lee−Yang−Parr,[31] with the standard 6-31+G* basis set has been used for geometry optimizations with no constrained degrees of freedom. It has been shown in the previous theoretical studies that the B3LYP approach with a basis set of double-ζ quality plus polarization functions can provide a reliable description for the gas-phase 1,3-DC reactions.[32,33] Vibrational frequencies, calculated at the B3LYP/6-31+G* level, have been used for characterization of stationary points. All of the stationary points have been positively identified as minima (number of imaginary frequencies, NIMAG = 0) or transition states (NIMAG = 1). Reported energies are zero-point corrected, unless otherwise specified. In addition, single-point calculations have been done at the selected critical points, using the 6-311+G(2df,p) basis set, to investigate the basis set effect on the reaction energetics.

A C_9H_{12} cluster model has been employed to represent a dimer site on the C(100)-2 × 1 surface. This cluster model in combination with the B3LYP density functional method was also used in the theoretical studies of the Diels−Alder cycloaddition of 1,3-butadiene on the C(100)-2 × 1 surface[16,17] and the reaction of HN_3 with the C(100)-2 × 1 surface.[34] For some cases, a $C_{21}H_{22}$ cluster representing three adjacent dimers from a single dimer row[16] has been used to investigate the effect of cluster size. All calculations were performed with the GAUSSIAN 94 package of programs.[35]

Results and Discussion

For the 1,3DCs of the 1,3-dipoles on the C_9H_{12} surface model, the fully optimized geometries of the reactants, transition states, and products are presented in Figures 1−4, respectively. The corresponding relative energies predicted at the B3LYP/6-31+G* level are given in Table 1. For comparison, the reaction energies and activation energies for the corresponding molecular reactions predicted at the same level of theory are also included in Table 1.

Transition-State Structures and Barrier Heights. The optimized transition states, TS_*n* (*n* = 1−7), for the 1,3-DCs on C_9H_{12} are shown in Figures 1−4, except for the case of O_3, which has no transition state. These are TS_1 for nitrile ylide, TS_2 for nitrile imine, TS_3 for nitrile oxide, TS_4 for diazomethane, TS_5 for methyl azide, TS_6 for nitrous oxide, and TS_7 for nitromethane. Each transition state has been confirmed by vibrational analysis that reveals the single imaginary frequency (i.e., 82i cm^{-1} for TS_1, 85i cm^{-1} for TS_2, 220i cm^{-1} for TS_3, 247i cm^{-1} for TS_4, 205i cm^{-1} for TS_5, 300i cm^{-1} for TS_6 and 232i cm^{-1} for TS_7). Further examination of the calculated imaginary normal mode of the transition states and more elaborate IRC (intrinsic reaction coordinate) calculations indicate that these transition states connect the corresponding reactants, 1,3-dipoles + C_9H_{12}, to the 1,3-DC products, and these 1,3-DC processes are concerted in nature.

The feature that the 1,3-DC follows a concerted pathway is also evidenced by the geometries of the transitions states. The lengths of the two newly forming bonds in each transition state are not deviated from each other too much, as shown in Figures 1−4. Further detailed comparison of the seven transition structures leads to the following remarks:

(i) All transition states are very early, as evidenced by the very large values of the two newly forming bond lengths that range from 2.223 Å for the C−O bond length in TS_7 to 2.903 and 2.968 Å for the two C−C bond lengths in TS_1.

(ii) The two newly forming bond lengths decrease in the following order: TS_1 of nitrile ylide (2.903 and 2.968

(25) *1,3-Dipolar Cycloaddition Chemistry*; Padwa, A., Ed.; John Wiley & Sons: New York, 1984; Vol. 1.
(26) Diederich, F.; Thilgen, C. *Science* **1996**, *271*, 317.
(27) Cases, M.; Duran, M.; Mestres, J.; Martin, N.; Sola, M. *J. Org. Chem.*, **2001**, *66*, 433 and references therein.
(28) Barriocanal J. A.; Doren, D. J. *J. Vac. Sci. Technol. A* **2000**, *18*, 1959.
(29) Barriocanal J. A.; Doren, D. J. *J. Phys. Chem. B* **2000**, *104*, 12269.
(30) Becke, A. D. *J. Chem. Phys.* **1993**, *98*, 5648.
(31) Lee, C.; Yang, W.; Parr, R. G. *Phys. Rev. A* **1988**, *37*, 785.
(32) Houk, K. N.; Wiest, O. *Top. Curr. Chem.* **1996**, *183*, 1.
(33) Su, M. D.; Liao, H. Y.; Chung, W. S.; Chu, S. Y. *J. Org. Chem.* **1999**, *64*, 6710.
(34) Lu, X.; Fu, G.; Wang, N.; Zhang, Q.; Lin, M. C.; *Chem. Phys. Lett.* **2001**, *343*, 212.
(35) Frisch, M. J.; Trucks, G. W.; Schlegel, H. B.; Gill, P. M. W.; Johnson, B. G.; Robb, M. A.; Cheeseman, J. R.; Keith, T.; Peterson, G. A.; Montgomery, J. A.; Raghavachari, K.; Al-Laham, M. A.; Zakrzewski, V. G.; Ortiz, J. V.; Foresman, J. B.; Peng, C. Y.; Ayala, P. Y.; Chen, W.; Wong, M. W.; Andres, J. L.; Replogle, E. S.; Gomperts, R.; Martin, R. L.; Fox, D. J.; Binkley, J. S.; Defrees, D. J.; Baker, J.; Stewart, J. P.; Head-Gordon, M.; Gonzalez, C.; Pople, J. A. *Gaussian 94, Revision B.3*; Gaussian, Inc.: Pittsburgh, PA, 1995.

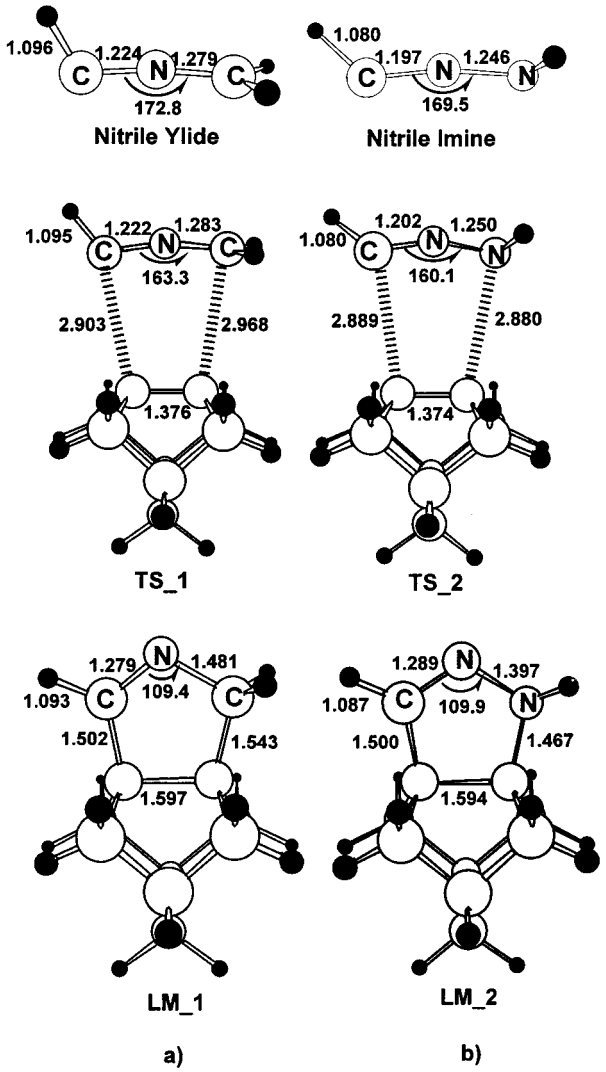

Figure 1. B3LYP/6-31+G*-optimized geometries (in Å and deg) of the reactants, transition states, and products of (a) nitrile ylide/C_9H_{12} and (b) nitrile imine/C_9H_{12}.

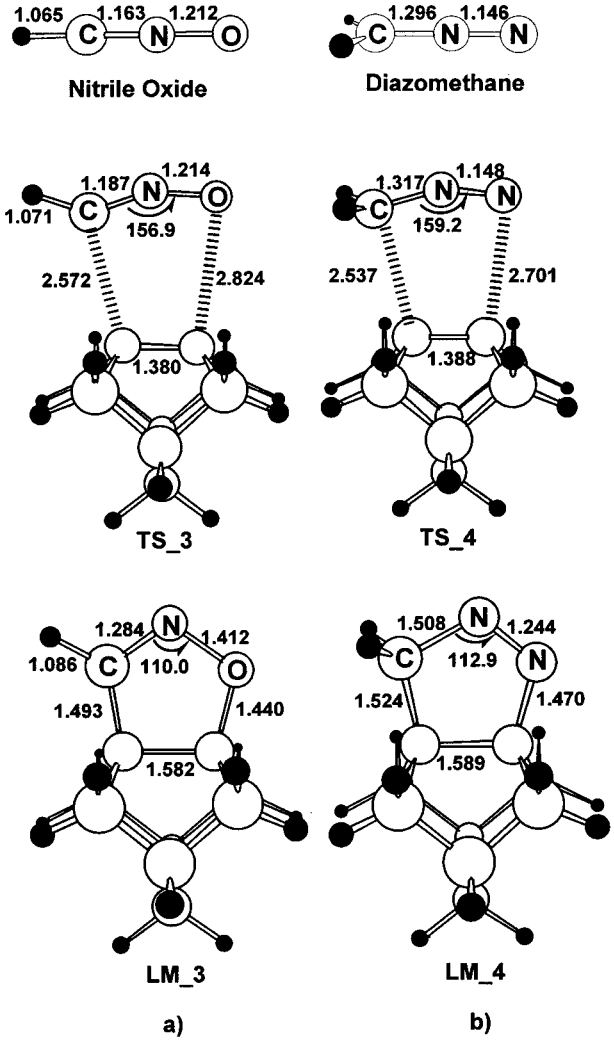

Figure 2. B3LYP/6-31+G*-optimized geometries (in Å and deg) of the reactants, transition states, and products of (a) nitrile oxide/C_9H_{12} and (b) diazomethane/C_9H_{12}.

Å) > TS_2 of nitrile imine (2.880 and 2.889 Å) > TS_3 of nitrile oxide (2.572 and 2.824 Å) > TS_4 of diazomethane (2.537 and 2.701 Å) > TS_5 of methyl azide (2.445 and 2.580 Å) and > TS_6 of nitrous oxide (2.327 and 2.475 Å) > TS_7 of nitromethane (2.223 and 2.223 Å).

(iii) Due to the approach of the 1,3-dipoles, the C═C bond length of the surface dimer in TS_*n* (*n* = 1−7) is slightly elongated, given the trend that the closer the 1,3-dipoles is, the longer the C═C bond length in the transition state. The extent of C═C bond elongation ranges from 0.010 Å for the nitrile imine case to 0.044 Å for the nitromethane case.

The above structural features indicate that the transition structures for the 1,3-dipoles with more electropositive atoms lying at the terminal positions are more reactant-like. This is consistent with the Hammond postulate,[36] which associates an earlier transition state with smaller reaction barrier and a larger exothermicity. As will be shown below, the 1,3-DC surface reaction with a more reactant-like transition structure does have a smaller activation barrier and a larger exothermicity.

The barrier heights predicted at the B3LYP/6-31+G* level for these 1,3DCs are given in Table 1. In accordance with the trends of transition-state structures, the barrier heights for the 16-valence-electron 1,3-dipoles increase in the order: TS_2 of nitrile imine (1.4 kcal mol^{-1}) ≈ TS1 of nitrile ylide (1.6 kcal mol^{-1}) < TS_3 of nitrile oxide (4.8 kcal mol^{-1}) and TS_4 of diazomethane (5.3 kcal mol^{-1}) < TS_5 of methyl azide (5.7 kcal mol^{-1}) < TS_6 of nitrous oxide (9.4 kcal mol^{-1}), indicating that the more electronegative the atom lying at the terminal positions of the 1,3-dipoles, the higher activation barrier for the 1,3-diploar cyclocation. More specifically, it can be seen that the activation barriers for the azo-type reactions are larger than those for the nitrile-type reactions, namely, diazomethane (CH_2NN) > nitrile ylide ($HCNCH_2$), methyl azide (CH_3NNN) > nitrile imine (HCNNH), and nitrous oxide (NNO) > nitrile oxide (HCNO). Previous theoretical study on the molecular 1,3-DC reactions revealed that the 16-valence-electron 1,3-dipole with more electropositive substituents at the terminals has a smaller HOMO−LUMO gap as well as a smaller energy splitting between its singlet and triplet states, which in turn facilitates its 1,3-DC reaction with a smaller activation barrier and a larger exothermicity.[33] The barrier height for the 1,3-DC of 18-valence-electron nitromethane is 7.8 kcal mol^{-1}

(36) Hammond, G. S. *J. Am. Chem. Soc.* **1954**, *77*, 334.

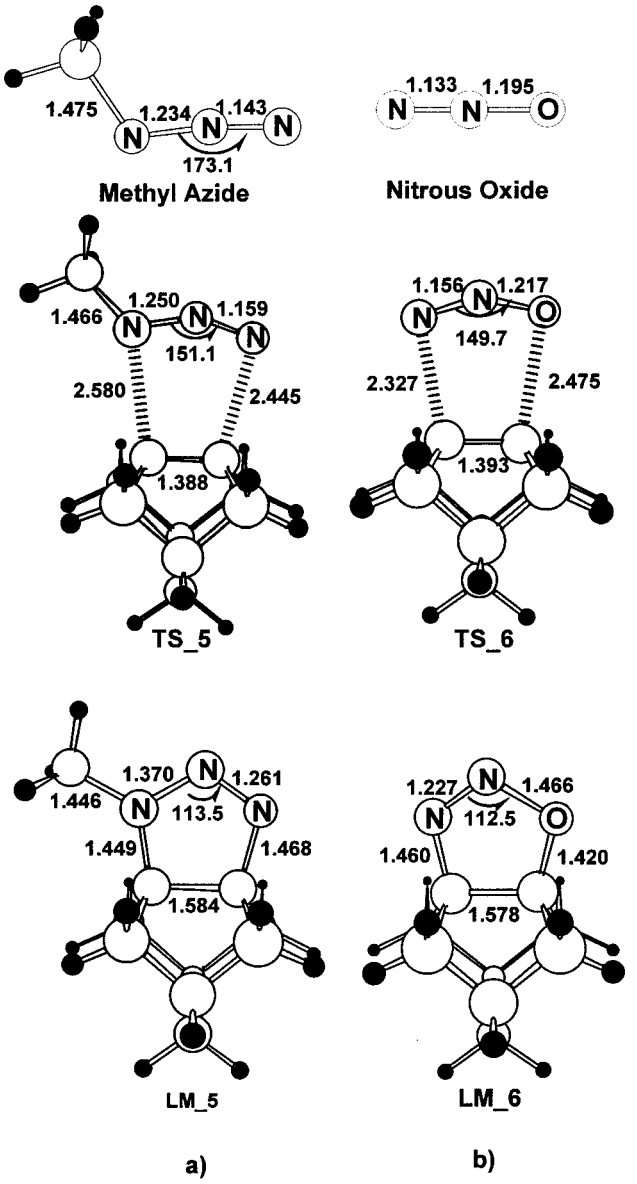

Figure 3. B3LYP/6-31+G*-optimized geometries (in Å and deg) of the reactants, transition states, and products of (a) methyl azide/C_9H_{12} and (b) nitrous oxide/C_9H_{12}.

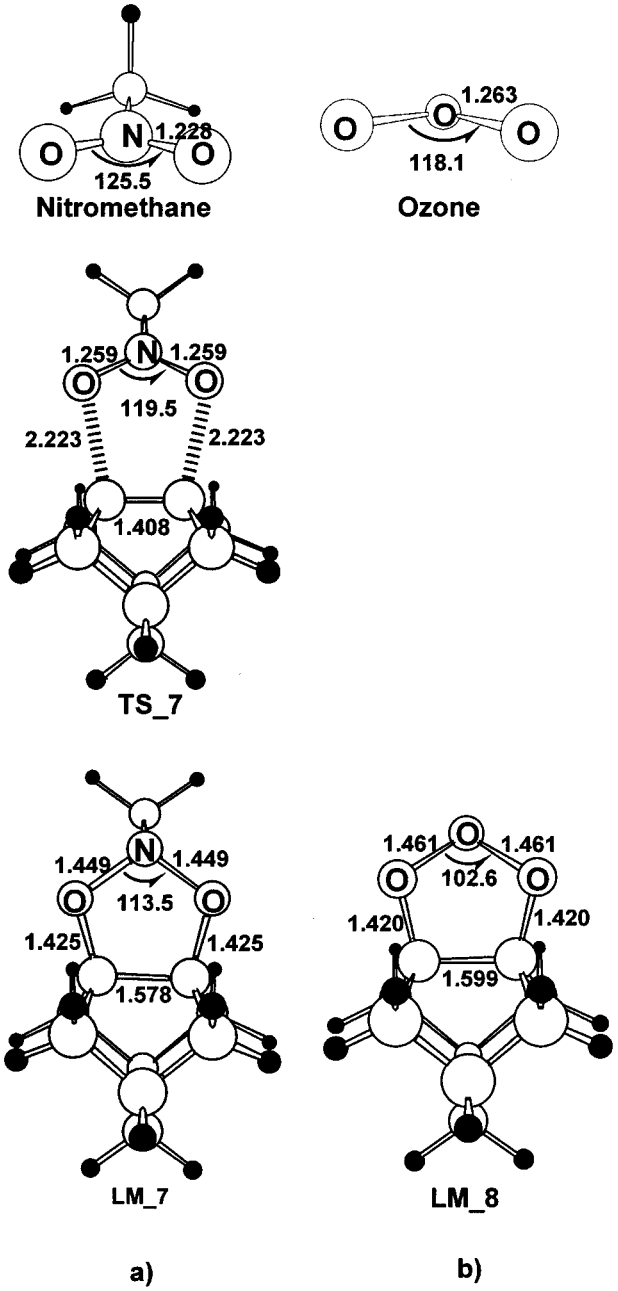

Figure 4. B3LYP/6-31+G*-optimized geometries (in Å and deg) of the reactants, transition states, and products of (a) nitromethane/C_9H_{12} and (b) ozone/C_9H_{12}.

predicted at the same level, while the 1,3-DC of another 18-valence-electron 1,3-dipole, ozone, is found to be barrierless. The barrier heights calculated by single-point B3LYP/6-311+G(2df,p) calculations are also given in Table 1. As it can be seen, the use of larger basis sets does not have a significant effect on the prediction of barrier height and does not alter the order of barrier height predicted at the B3LYP/6-31+G* level.

For the sake of comparison, we have also calculated the transition states for the 1,3-DCs of the eight 1,3-dipoles with ethylene at the B3LYP/6-31+G* level. The optimized transition states, which are not given here, resemble those of the surface reactions but have shorter intermolecular bond lengths than have those of the surface reactions. As such, the transition states for the molecular 1,3-DCs are later than their surface reaction analogues. Another evidence of this remark is that the calculated imaginary frequencies for the transition states of the molecular 1,3DCs are far larger than those of the surface 1,3-DCs, as shown in Table 1.

So far as the barrier height is concerned, the molecular 1,3-DCs have far larger values of barrier heights than have the surface 1,3-DCs. As shown in Table 1, the difference in the barrier height of the molecular and surface 1,3-DCs ranges from 6.6 kcal mol^{-1} for the nitrile imine case to 20.1 kcal mol^{-1} for the nitromethane case. Hence, it is evidenced that the surface 1,3-DCs are kinetically more favorable than their molecular analogues. Conclusively, the reactivity of the 16-valence-electron 1,3-dipoles toward the surface dimer follows the same order of reactivity that they display toward ethylene: nitrile ylide ≈ nitrile imine > nitrile oxide > diazomethane > methyl azide > nitrous oxide. A similar trend is followed by the 18-valence-electron 1,3-dipoles, i.e., ozone > nitromethane. Among all the 1,3-dipoles concerned, ozone is the most reactive with the surface

Table 1. Reaction Energies (ΔE_r in kcal mol^{-1}) and Energy Barriers (ΔE_a in kcal mol^{-1}) of the 1,3-DC Reactions of 1,3-Dipoles with the C_9H_{12} Surface Model and C_2H_4 (the Imaginary Frequencies (ν_i in cm^{-1}) of Transition States Are Also Presented)

		C_9H_{12}			C_2H_4				
1,3-dipole	method	ΔE_r	ΔE_a	ν_i	ΔE_r	ΔE_a	ν_i	ΔE_{rr}[a]	ΔE_{aa}[b]
$HCNCH_2$	B3LYP/6-31+G*	−106.7	1.6	82i	−63.2	8.7	382i	43.5	7.1
	B3LYP/6-311+G(2df,p)	−103.3	1.5						
HCN_2H	B3LYP/6-31+G*	−100.8	1.4	85i	−55.2	8.0	353i	45.1	6.6
	B3LYP/6-311+G(2df,p)	−96.4	1.7						
HCNO	B3LYP/6-31+G*	−86.4	4.8	220i	−38.7	13.0	401i	47.7	8.2
	B3LYP/6-311+G(2df,p)	−81.7	5.6						
CH_2N_2	B3LYP/6-31+G*	−75.1	5.3	247i	−30.1	16.1	451i	45.1	10.8
	B3LYP/6-311+G(2df,p)	−70.0	6.0						
CH_3N_3	B3LYP/6-31+G*	−69.7	5.7	205i	−22.9	17.7	406i	46.8	12.0
	B3LYP/6-311+G(2df,p)	−64.7	7.2						
N_2O	B3LYP/6-31+G*	−56.9	9.4	300i	−7.0	24.2	458i	49.9	14.8
	B3LYP/6-311+G(2df,p)	−51.7	11.4						
CH_3NO_2	B3LYP/6-31+G*	−46.9	7.8	232i	+1.9	27.9	522i	48.8	20.1
	B3LYP/6-311+G(2df,p)	−44.1	9.2						
O_3	B3LYP/6-31+G*	−109.9	- -	- -	−56.6	−1.8[c]	150i	53.3	- -
	B3LYP/6-311+G(2df,p)	−107.7							

[a] $\Delta E_{rr} = \Delta E_r(C_2H_4) - \Delta E_r(C_9H_{12})$ (kcal mol^{-1}). [b] $\Delta E_{aa} = \Delta E_a(C_2H_4) - \Delta E_a(C_9H_{12})$ (kcal mol^{-1}). [c] A precursor complex of (O_3+ C_2H_4) is predicted with a binding energy of −2.6 kcal mol^{-1}.

dimer, as demonstrated by its barrierless 1,3-DC on the C_9H_{12} surface model.

1,3-DC Products and Energies. All 1,3-DCs studied here produce five-membered ring surface species. The optimized geometries for the 1,3-DC products, LM_*n* (*n* = 1−8), are also depicted in Figures 1−4, respectively. These are LM_1 for nitrile ylide, LM_2 for nitrile imine, LM_3 for nitrile oxide, LM_4 for diazomethane, LM_5 for methyl azide, LM_6 for nitrous oxide, LM_7 for nitromethane, and LM_8 for ozone.

In the 1,3-DC products, the two newly formed intermolecular bond lengths vary with the nature of the bonds, i.e., the C−C bond length ranges from 1.493 Å in LM_3 to 1.543 Å in LM_1, the N−C bond length ranges from 1.449 Å in LM_5 to 1.470 Å in LM_4, and the O−C bond length ranges from 1.420 Å for LM_8 to 1.440 Å for LM_6. These bond lengths are typical for the X−C (X = C, N, O) single bonds and follow the trend that the more electronegative of the X atom, the shorter the X−C bond. In particular, the C−C bond with a C atom adopting the sp^2 hybridization (∼1.50 Å) is by ∼0.4 Å shorter than the one with both C atoms adopting the sp^3 hybridization (∼1.54 Å). On the other hand, it is known that the bond order of the dipolarophile decreases upon 1,3-DC. As a result, the C=C bond length of the surface dimer increases considerably due to the 1,3-DCs. In the 1,3-DC products, the C−C bond length of the surface dimer ranges within 1.578−1.599 Å, which is typical for a C−C single bond.

At the B3LYP/6-31+G* level, the 1,3-DCs of the eight 1,3-dipoles on the C_9H_{12} are predicted to be highly exothermic, in accordance with the presence of much earlier transition states. The exothermicity ranges from −46.9 kcal mol^{-1} for the nitromethane case to −109.7 kcal mol^{-1} for the ozone case. For the 16-valence-eletron 1,3-dipoles, the 1,3-DC exothermicity follows the order nitrile ylide (−106.7 kcal mol^{-1}) > nitrile imine (−100.8 kcal mol^{-1}) > nitrile oxide (−86.4 kcal mol^{-1}) > diazomethane (−75.1 kcal mol^{-1}) > methyl azide (−69.7 kcal mol^{-1}) > nitrous oxide (−56.9 kcal mol^{-1}), in good accordance with the reverse order of their barrier heights. That is, the 1,3-DC with lower barrier height has higher exothermicity, in agreement with the Hammond postulate.[36] Single-point B3LYP/6-311+G(2df,p) calculations do not alter the above trend. As shown in Table 1, the exothermicity predicted at the B3LYP/6-311+G(2df,p) level is only 2−5 kcal mol^{-1} lower than that predicted at the B3LYP/6-31+G* level.

We have also calculated the exothermicity for the gas-phase 1,3-DCs of these eight 1,3-dipoles with ethylene. The reaction energies predicted at the B3LYP/6-31+G* level are given in Table 1. It can be seen that for each 1,3-dipole concerned, the surface 1,3-DC is thermodynamically much favorable over its molecular analogue; the difference in the reaction energy of the surface and molecular 1,3-DCs, ΔE_{rr}, ranges from 43.5 kcal mol^{-1} for nitrile ylide to 55.3 kcal mol^{-1} for ozone. Meanwhile, the difference in activation energy of the surface and molecular 1,3DCs, ΔE_{aa}, ranges from 6.6 kcal mol^{-1} for nitrile imine to 20.1 kcal mol^{-1} for nitrous oxide, except for the case of ozone. The facileness of the surface reactions with respect to their molecular analogues can be attributed to the weaker π-bonding in surface dimer than that in ethylene. Note that the π-bond strength on C(100) (∼28 kcal mol^{-1})[37] is ∼30 kcal mol^{-1} smaller than that for ethylene (∼56 kcal mol^{-1}).[38] Such a concept can be readily extended to the understanding of the quite high reactivity of the Si(100)-2 × 1 surface toward 1,3-dipoles,[28] as the π-bond strength on Si(100) is estimated to be only 5∼10 kcal mol^{-1},[39] even weaker than that of the C(100)-2 × 1 surface. Theoretically, it was predicted that the 1,3-DC of diazomethane onto the Si(100)-2 × 1 surface is barrierless.[28] In addition, it should be noted that in organic chemistry, the 1,3-DC products sometimes might undergo further isomerization or decomposition.[25,40] For example, the 1,3-DC product of (diazomethane + ethylene) can be easily decomposed into N_2 and cyclopropane, due to the high stability of N_2.[25,41] Similar N_2 elimination was also found from the 1,3-DC product of (methyl azide + ethylene).[25] Even more complex decomposition products

(37) Hukka, T. J.; Pakkanen, T. A.; D'Evelyn, M. P. *J. Phys. Chem.* **1994**, *98*, 12420.
(38) Mchurry, J. *Organic Chemistry*, 4th ed.; Brooks/Cole Publishing Co.: Pacific Grove, 1996; p 23.
(39) Doren, D. J. *Adv. Chem. Phys.* **1996**, *95*, 1.
(40) March, J. *Advanced Organic Chemistry*, 4th ed.; Wiley: New York, 1992; p 1045 and references therein.
(41) Neeb, P.; Horie O.; Moortgat G. K. *J. Phys. Chem. A* **1998**, *102*, 6778.

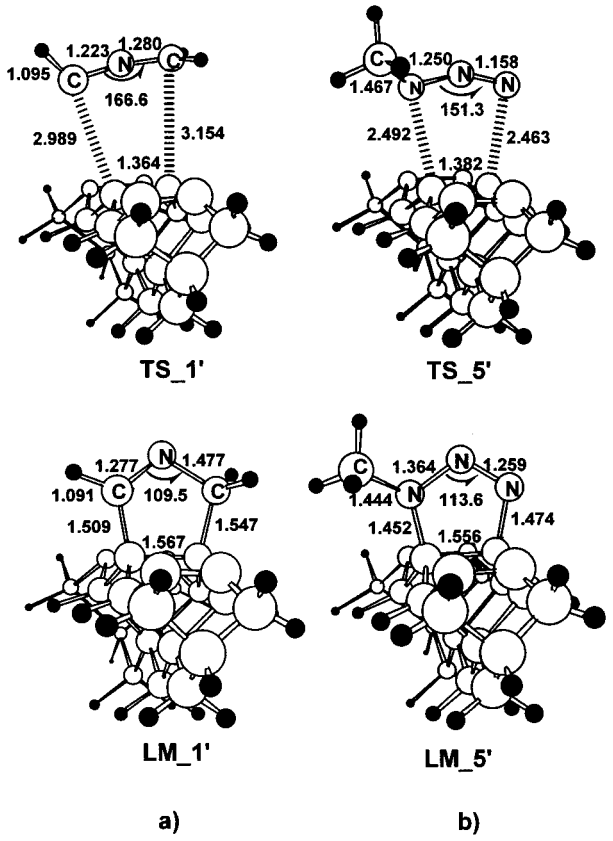

Figure 5. B3LYP/6-31+G*-optimized geometries (in Å and deg) of the reactants, transition states, and products of (a) nitrile ylide/$C_{21}H_{22}$ and (b) methyl azide/$C_{21}H_{22}$.

were encountered from the 1,3-DC product of (ozone + ethylene).[41,42] For the 1,3-DC reactions on C(100) surface, one expects that somewhat similar decomposition or isomerization processes might occur on the 1,3-DC products. For methyl azide and diazomethane on C(100) surface, the 1,3-DC products, i.e., LM_5 for methyl azide and LM_3 for diazomethane, may be thermally decomposed, leading to N_2 elimination and the formation of three-membered ring surface species. For ozone, the 1,3-DC product, LM_8, may be decomposed to produce $O_2(^1\Delta_g)$ and epoxy surface species. Details of the decomposition mechanism for the 1,3-DC products are being explored and will be reported elsewhere.

(42) Anglada, J. M.; Crehuet, R.; Bofill, J. M. *Chem. Eur. J.* **1999**, *5*, 1809.

Cluster Size Effect. To show how the predicted reaction energetics depend on the size of cluster, we have also investigated the 1,3-DC reactions of, for example, nitrile ylide and methyl azide with the middle dimer of the triple-dimer model, $C_{21}H_{22}$, at the B3LYP/6-31+G* level of theory. However, no significant size effect on the reaction energetics is found for either case. For methyl azide on $C_{21}H_{22}$, the predicted activation energy and reaction energy are 5.7 and −64.0 kcal mol^{-1}, respectively, agreeing well with the values of 5.7 and −69.7 kcal mol^{-1} obtained by using C_9H_{12} cluster. For nitrile ylide on $C_{21}H_{22}$, the predicted activation energy and reaction energy are 1.0 and −102.6 kcal mol^{-1}, respectively, in accordance with the values of 1.6 and −106.7 kcal mol^{-1} predicted for nitrile ylide on C_9H_{12}. The optimized geometries for transition states and products of the nitrile yilide/$C_{21}H_{22}$ and methyl azide/$C_{21}H_{22}$ systems are given in parts a and b, respectively, of Figure 5, which are comparable with those depicted in Figures 1a and 3a.

Conclusion

The 1,3-dipolar cycloadditions of a series of 1,3-dipolar molecules onto the C(100)-2 × 1 surface have been investigated by means of hybrid density functional B3LYP method in combination with cluster model approach. It was found that 1,3-DCs on the C(100)-2 × 1 surface are much favorable over their molecular analogues both thermodynamically and kinetically. The enhancement of the reactivity on the surface can be attributed to the reduced overlap between the p_π orbitals of the surface C═C dimer. The facileness of this new type of surface reactions should be important for the semiconductor industry because it might lead to a breakthrough in the fabrication of diamond films at low temperature.

Acknowledgment. This work was supported by the Natural Science Foundation of China, the Education Ministry of China, the Fok Ying-Tung Educational Foundation, and Xiamen University.

Supporting Information Available: Cartesian coordinates of all reported stationary points, as well as the total electronic and zero-point vibrational energies. This material is available free of charge via the Internet at http://pubs.acs.org.

JO016114Q